ELSEVIER

Biochimica et Biophysica Acta 1240 (1995) 237–247

BBA Biochimica et Biophysica Acta

Lateral domain formation in cholesterol/phospholipid monolayers as affected by the sterol side chain conformation

Peter Mattjus [a,*], Robert Bittman [b], Catherine Vilchèze [b], J. Peter Slotte [a]

[a] *Department of Biochemistry and Pharmacy, Åbo Akademi University, FIN-20520 Turku, Finland*
[b] *Department of Chemistry and Biochemistry, Queens College of The City University of New York, Flushing, NY 11367-1597, USA*

Received 12 May 1995; accepted 3 August 1995

Abstract

The interaction of side-chain variable cholesterol analogues with dipalmitoylphosphatidylcholine (DPPC) or *N*-palmitoylsphingomyelin (*N*-PSPM) has been examined in monolayer membranes at the air/water interface. The sterols had either unbranched (*n*-series) or single methyl-branched (*iso*-series) side chains, with the length varying between 3 and 10 carbons (C3–C10). The efficacy of interaction between the sterols and the phospholipids was evaluated based on the ability of the sterols to form condensed sterol/phospholipid domains in the phospholipid monolayers. Domain formation was detected with monolayer fluorescence microscopy using NBD-cholesterol as the fluorescent probe. In general, a side chain length of at least 5 carbons was necessary for the unbranched sterols to form visible sterol/phospholipid domains in DPPC or *N*-PSPM mixed monolayers. With the *iso*-analogues, a side chain of at least 6 carbons was needed for sterol/phospholipid domains to form. The macroscopic domains were stable up to a certain surface pressure (ranging from 1 to 12 mN/m). At this onset phase transformation pressure, the domain line boundary dissipated, and the monolayer entered into an apparent one phase state (no clearly visible lateral domains). However, with some DPPC monolayers containing short chain sterols (*n*-C3, *n*-C4,*n*-C5, and *i*-C5), a new condensed phase appeared to form (at 20 mol%) when the monolayer was compressed beyond the phase transformation pressure. These precipitates formed at surface pressures between 6–8.3 mN/m, were clearly observable up to at least 30 mN/m. When the monolayers containing these four sterols were allowed to expand, the condensed precipitates dissolved at the same pressure at which they were formed during monolayer compression. No condensed precipitates were observed with these sterols in corresponding *N*-PSPM monolayers. Taken together, the results of this study emphasize the importance of the length and conformation of the cholesterol side chain in determining the efficacy of sterol/phospholipid interaction in model membranes. The major difference between DPPC and *N*-PSPM monolayers at different sterol compositions was mainly the lateral distribution and the size of the domains as well as the onset phase transformation pressure intervals.

Keywords: Sterol side chain; Cholesterol; Phosphatidylcholine; Sphingomyelin; Monolayer membrane; Sterol–phospholipid interaction; Lipid domain

1. Introduction

The structure of the cholesterol molecule has evolved to include unique functions and properties as a membrane component. This special molecular structure gives cholesterol its amphiphilic character which allows for molecular interactions with different types of phospholipids, e.g., phosphatidylcholines and sphingomyelins. The presence of cholesterol in the plasma membrane modulates the general lipid environment and also regions close to integral proteins [1]. The important amphiphilic character of cholesterol is provided by the hydrophilic 3β-hydroxy group, by the hydrophobic tetracyclic ring structure, and by the isooctyl side chain at position C-17. This side chain seems to give the molecule essential properties for interactions with phospholipids [2,3]. 5-Androsten-3β-ol, which lacks the isooctyl side chain, can neither condense dipalmitoylphosphatidylcholine (DPPC) monolayers [2,4], nor reduce the solute permeability of phosphatidylcholine liposomes [5]. Sterols having shorter or longer side chains (as compared to the isooctyl chain of cholesterol) are also less effective as rigidifiers in phospholipid bilayer membranes than cholesterol [6–8]. In addition, polyene antibiotics like

Abbreviations: PC, phosphatidylcholine; SPM, sphingomyelin; DPPC, 1,2-dipalmitoyl-*sn*-glycero-3-phosphocholine; *N*-PSPM, *N*-palmitoyl-D-sphingomyelin; NBD-cholesterol, 22-(*N*-(7-nitrobenz-2-oxa-1,3-diazol-4-yl)amino)-23,24-bisnor-5-cholen-3β-ol.

* Corresponding author. Fax: +358 21 2654745; e-mail: pmattjus@abo.fi.

SSDI 0005-2736(95)00179-4

amphotericin B and filipin interact differently with sterols in small unilamelar vesicles, depending on the sterol side-chain structure [9]. The transbilayer movement of sterols across the membrane bilayer of growing mycoplasma cells [10], as well as the intestinal absorption of sterols [11] and the rate of spontaneous sterol movement between vesicles or between lyso-PC dispersions [12,13], have also been shown to depend on the side chain composition. A recent study from this laboratory, using cholesterol oxidase to probe for the strength of sterol-phospholipid interaction, reported a significant difference in sterol/phospholipid interaction in both monolayers and small unilamellar vesicles as a function of the sterol side chain composition [4].

The difference in molecular interactions between cholesterol and phosphatidylcholine on one hand and sphingomyelin on the other has recently been examined by several research groups using a variety of different techniques ([14], and references therein). The most apparent difference between phosphatidylcholine and sphingomyelin regarding their interaction with cholesterol appears to reside in their different capacity to solubilize cholesterol [15,16]. The difference in the solubilizing properties of the two phospholipids is also sensed by techniques that measure the relative strength of molecular interaction between the phospholipid and cholesterol (i.e., cholesterol oxidase; [14,15]). Our recent monolayer studies have shown that the amide function of sphingomyelin is in part responsible for the increased affinity between cholesterol and sphingomyelin [17]. At present it is not known how sensitive the cholesterol/sphingomyelin interaction is to alterations in the sterol side chain composition.

Another measure of the specific sterol/phospholipid interaction in membranes is the formation of laterally segregated sterol-rich domains in a bulk of a phospholipid-rich phase [18,19]. Monomolecular lipid films at the air/water interface have been visualized with monolayer fluorescence microscopy (for a review, see [20]). Laterally condensed domains in a 'sea' of a laterally expanded phase can be directly observed, since a suitable fluorophore present in the membrane partition differently into these two lateral phases [21,22]. The fluorescent probe NBD-cholesterol used in this study has been shown to partition preferentially into a expanded phases, and is consequently excluded from more condensed phases [23].

In this study we have examined the formation of lateral sterol-rich domains in mixed sterol/phospholipid monolayers using monolayer fluorescence microscopy. Our objective was to examine the effect of the sterol side chain composition on the formation of sterol-rich domains. We have used a number of sterol analogues which have either an unbranched (*n*-series) or a single methyl-branched (*iso*) side chain of different length (from 3 to 10 carbons). A further comparison was made between DPPC and *N*-palmitoylsphingomyelin (*N*-PSPM), since the affinity of interaction between a sterol and these two phospholipids appears to differ.

2. Experimental procedures

2.1. Materials

Cholesterol, DPPC and *N*-PSPM were obtained from Sigma (St. Louis, MO). NBD-cholesterol (22-(*N*-(7-nitrobenz-2-oxa-1,3-diazol-4-yl)amino)-23,24-bisnor-5-cholen-3β-ol) was purchased from Molecular Probes (Eugene, OR). The sterol analogues were prepared as described previously [4]. Each compound gave a single spot when analyzed by thin-layer chromatography. Stock solutions of sterols, phospholipids, and NBD-cholesterol were prepared in hexane/2-propanol (3:2, v/v), and stored in the dark at −25°C. The water was purified with reverse osmosis, and further passed through a Milli-Q UF + filtering system to a resistivity better than 18 MΩ/cm.

2.2. Monolayer preparation and visualization

The solutions containing the sterol and either PC or SPM were prepared immediately prior to spreading. 30 nmol of appropriate lipids, containing 1 mol% NBD-cholesterol, were spread with a Hamilton syringe on the air/water interface in a Teflon-milled trough. The monolayer was allowed to stabilized for about 2 min after which it was subjected to symmetric compression at a speed not

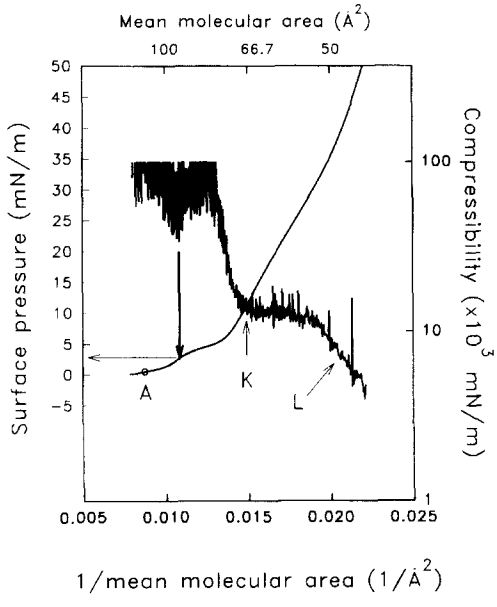

Fig. 1. Force–area isotherm of 20 mol% cholesterol in DPPC at 22°C. The isotherm is plotted as the inverse molecular area versus surface pressure (smooth line), or as the inverse molecular area versus the logarithmic compressibility function (noisy line). The left-most deviation in the inverse compressibility function (down arrow) corresponds to the phase transformation pressure which also can be visually observed (cf. Figs. 3 and 7). The other discontinuities (K and L according to the nomenclature of Albrecht et al. [25]) indicate occurrences of lateral phase transitions in the monolayer. Mark A on the isotherm indicates the surface pressure (0.5 mN/m) at which the micrographs of Figs. 2, 4, 6, and 8 were documented during initial compression.

exceeding 4 Å^2/molecule per min. A KSV Minisystems (KSV Instruments, Helsinki) surface barostat mounted on an Olympus IMT-2 microscope was used, and the documentation of the monolayer morphology was accomplished using a Hitachi video camera connected to a DT3851 digitizing board (Data Translations, Marlboro, MA). At least three different runs were performed at each lipid composition, and representative micrographs were chosen from a number of similar images. Monolayer compressibility was calculated from the force–area isotherm function as described previously [24].

3. Results

The mixed monolayers were spread to an available mean molecular area of 133.5 Å^2, after which they were compressed to 40 mN/m, and then expanded to give a lateral surface pressure close to zero. Monolayer surface texture was documented at different stages during the compression, and after the expansion. Fig. 1 shows a force–area isotherm for 20 mol% cholesterol in DPPC at 22°C, and also indicates different regions of interest with regard to the experiments of this study. The mixed mono-

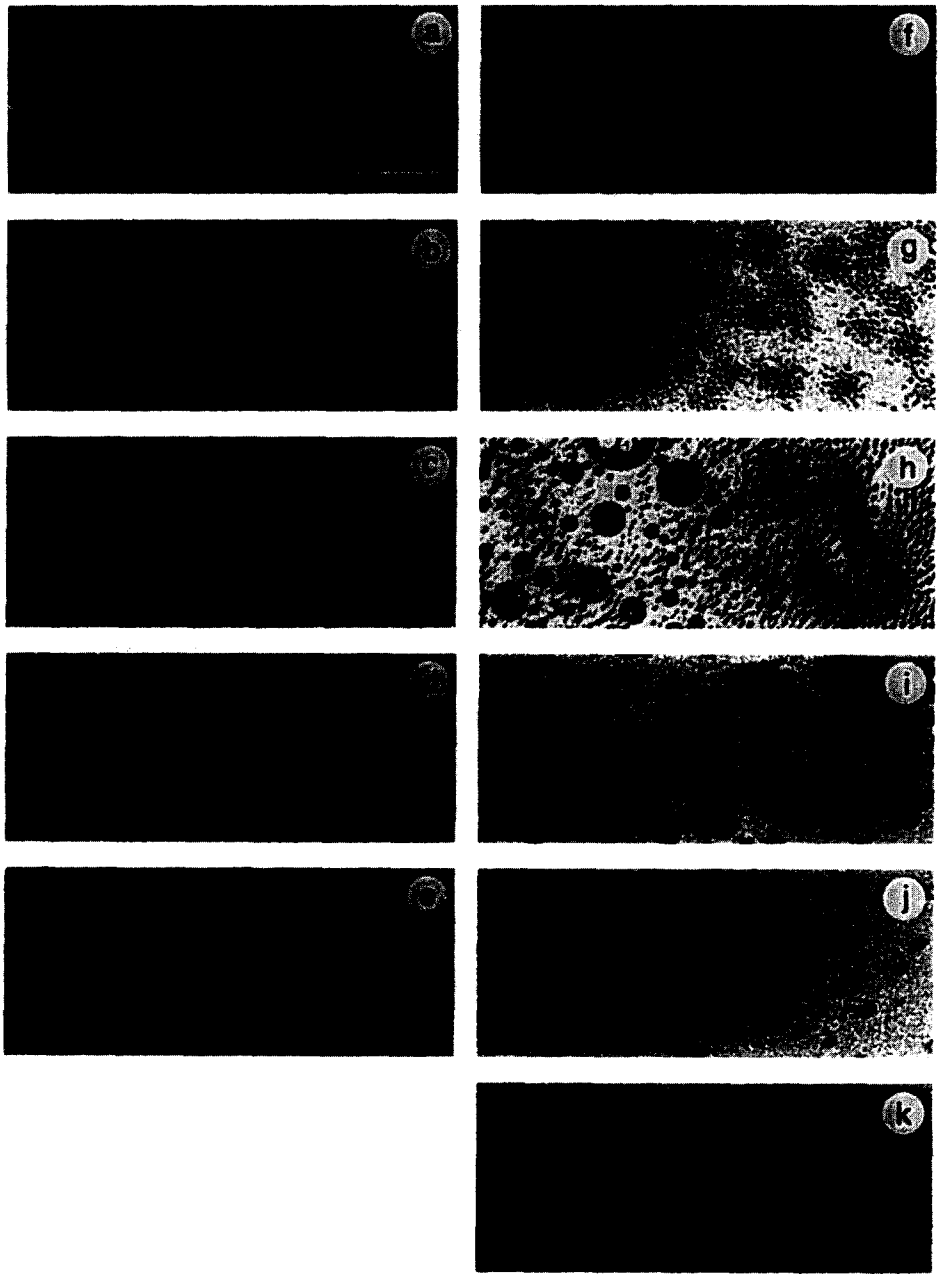

Fig. 2. Lateral domain formation in sterol/DPPC monolayers. The monolayers contained 20 mol% sterol, 79 mol% DPPC, and 1 mol% NBD-cholesterol. Micrographs were documented at 0.5 mN/m during the initial compression of the monolayer. Panel a is *n*-C3, b is *n*-C4, c is *n*-C5, d is *n*-C6, e is *n*-C7, f is *i*-C5, g is *i*-C6, h is *i*-C7, i is *i*-C8 (cholesterol), j is *i*-C9, and k is *i*-C10. The scale bar is 100 μm.

layer containing sterol and phospholipid was spread at an available mean molecular area of 133.5 Å^2. The monolayer was slowly compressed until the surface pressure reached a value of 0.5 mN/m (point A in Fig. 1). At this point the documentation was performed (Fig. 2, Fig. 4, Fig. 6, Fig. 8). At a surface pressure of 0.5 mN/m, cholesterol-rich condensed domains could be seen to coexist with an expanded phospholipid-rich phase. When the monolayer was compressed further, one reached a characteristic surface pressure at which the two-phase coexistence apparently disappeared (marked by a bold arrow in Fig. 1). At this point the mixed monolayer entered an apparent one phase state (as determined microscopically by visual observation). This characteristic surface pressure is termed the phase transformation pressure. The phase transformation pressure can also be deduced from an analysis of the force–area isotherm, if the inverse mean molecular area is plotted as a function of the logarithmic compressibility function (Fig. 1; cf. [25,26]). The point of phase transformation pressure can be approached both from a low or a high surface pressure. If one approaches the phase transformation pressure from the apparent one phase region (at a surface pressure above the phase transformation pressure), the monolayer will again enter a multiple phase coexistence state. The domain properties in monolayers which had experienced a compression/expansion cycle were also documented at 0.5 mN/m (but no micrographs are shown due to space limitation). The domains observed after a compression/expansion cycle may represent thermodynamically more stable structures [18,27,28].

3.1. Domain formation in sterol / DPPC monolayers

Monolayers containing 20 mol% sterol in DPPC (together with 1 mol% NBD-cholesterol) were prepared, spread, and compressed to 0.5 mN/m. Sterol analogues with different side-chain structures and lengths showed marked differences in their capacity to form sterol-rich lateral (condensed) domains in the mixed monolayers. With the unbranched side chain analogues, a uniformly fluorescent monolayer was seen with *n*-C3 and *n*-C4 sterols (Fig. 2a and b), indicating no formation of macroscopic sterol/phospholipid domains. The analogues *n*-C5, *n*-C6 and *n*-C7 formed clearly visible sterol/DPPC domains in the plane of the monolayer (Fig. 2c, d, and e). The condensed domains in these monolayers appeared to increase in size with increasing side chain length. Of the sterols having a branched side chain, both the *i*-C5 and the *i*-C10 failed to form laterally condensed domains (Fig. 2f and k), whereas the other branched sterols formed condensed domains. The *i*-C6 analogue formed small condensed domains which were aggregated in clusters (Fig. 2g), whereas larger and partly fused condensed domains could be seen in the *i*-C7 and *i*-C8 (cholesterol) mixed monolayers (Fig. 2h and i). The condensed domains became smaller again when the branched side chain length increased to from 8 to 9 carbons (Fig. 2j).

The structure of the sterol/DPPC domains were further examined in monolayers which had experienced a compression/expansion cycle, since condensed domains in such films may be closer to thermodynamic equilibrium. The size distribution of the condensed domains in the *n*-C5 monolayer was more uniform after the compression/expansion cycle, whereas the domains in the *n*-C6 and *n*-C7 monolayers were partly fused (micrographs not shown). With the *iso*-sterols, both the size and the lateral distribution of the condensed domains became more uniform after the compression/expansion cycle.

The onset phase transformation pressure at which the domain boundary line between condensed and expanded phases dissipated was also dependent on the sterol side chain composition. The onset phase transformation pressure found in monolayers with unbranched sterols was similar (1–1.4 mN/m) to that of monolayers from the three sterols that formed sterol/phospholipid domains (*n*-C5, *n*-C6 and *n*-C7; Fig. 3A solid line), whereas it de-

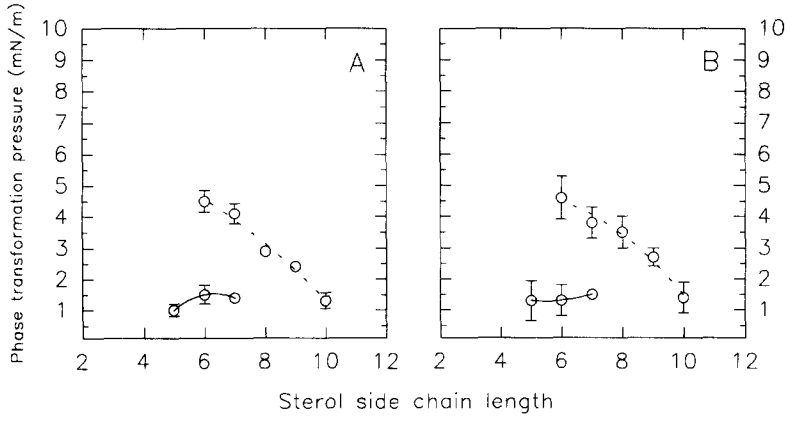

Fig. 3. Onset phase transformation pressure as a function of sterol side chain composition. Sterol/DPPC mixed monolayers were prepared to contain either 20 (panel A) or 33 (panel B) mol% sterol (together with 1 mol% NBD-cholesterol). The solid line represents sterols from the *n*-series, whereas dotted lines represent *iso*-sterols. Values are averages ± S.E. from three different experiments.

creased (from 4.5 to 1.3 mN/m) with increasing side chain length with the branched side chain analogues (Fig. 3A, dotted line).

At 33 mol% sterol in the mixed monolayers, *n*-C3 and *n*-C4 again failed to form discrete condensed domains with DPPC (during initial compression, at 0.5 mN/m; Fig. 4a and b). With longer chain unbranched analogues (*n*-C5, *n*-C6 and *n*-C7) the monolayer surface texture was dark with occasional (*n*-C5 and *n*-C7) or numerous (*n*-C6) brightly fluorescent inclusions (Fig. 4c–e). Of the single methyl branched analogues, the *i*-C5 failed to form lateral domains (Fig. 4f), whereas the other sterol formed a characteristic surface texture. The surface texture was foam-like with the *i*-C6 to *i*-C9 analogues (Fig. 4g–j), while the monolayer with the *i*-C10 had a surface texture which was characterized by small brightly fluorescent domains against a darker background (Fig. 4k). The monolayer surface texture after a compression/expansion cycle did not markedly change for the unbranched sterols, whereas the foamy texture of the *iso*-analogues became more homogenous (laterally expanded droplets against a condensed phase). The surface texture of the *i*-C9 and

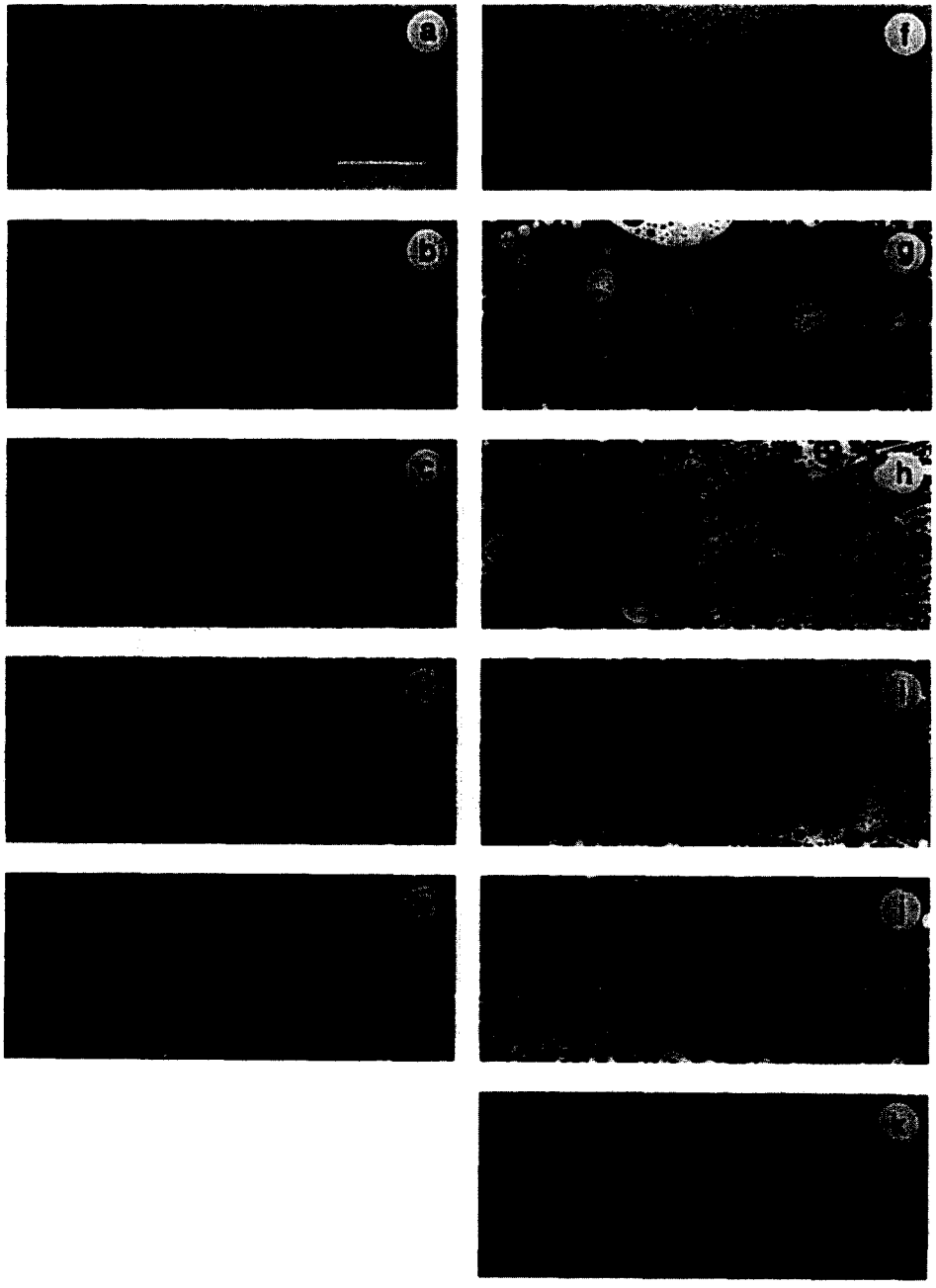

Fig. 4. Lateral domain formation in sterol/DPPC monolayers. The monolayers contained 33 mol% sterol, 66 mol% DPPC, and 1 mol% NBD-cholesterol. Micrographs were documented at 0.5 mN/m during the initial compression of the monolayer. Panel a is *n*-C3, b is *n*-C4, c is *n*-C5, d is *n*-C6, e is *n*-C7, f is *i*-C5, g is *i*-C6, h is *i*-C7, i is *i*-C8 (cholesterol), j is *i*-C9, and k is *i*-C10. The scale bar is 100 μm.

i-C10 monolayers was only marginally altered by the compression/expansion cycle. The onset phase transformation pressure observed at 33 mol% sterol was very similar to that observed at 20 mol% sterol (Fig. 3B and A).

When certain sterol/DPPC mixtures were compressed beyond the phase transformation pressure, the apparent one phase monolayer again turned into a two-phase coexistence at higher surface pressures. This phenomenon was observed with the *n*-C3, *n*-C4, *n*-C5 and *i*-C5 analogues at 20 mol% in DPPC. Of these, only *n*-C5 formed sterol-rich domains with DPPC at 0.5 mN/m during initial compression (Fig. 2c). The formation of laterally condensed precipitates in the *n*-C5/DPPC monolayer is shown in Fig. 5. The condensed domains present at 0.5 mN/m during initial compression (Fig. 5A, 0.45 mN/m) were dissolved when the monolayer was compressed beyond the phase transformation pressure of this mixture (Fig. 5B, 2.0 mN/m). When the apparently homogeneous monolayer was compressed further, a new dark phase formed at about 7.5 mN/m (Fig. 5C, micrograph taken at 10.4 mN/m). These condensed domains were present even at high surface pressures (Fig. 5D, 30 mN/m). When the monolayer was allowed to expand, the condensed domains adhered to each other, forming string-like aggregates (Fig. 5E, 10.5 mN/m). Below 7.5 mN/m, the precipitate dissolved and the monolayer was again apparently homogeneous (Fig. 5F, 2.0 mN/m). Below the phase transformation pressure, the sterol-rich domains reformed (Fig. 5G, 0.5 mN/m). The new phase (which appeared above the phase transformation pressure) was formed at a lateral surface pressure of 6 mN/m, 6.9 mN/m, 7.3 mN/m, and 8.3 mN/m for *n*-C3, *n*-C4, *n*-C5, and *i*-C5, respectively.

3.2. Domain properties in sterol / N-PSPM monolayers

Mixed monolayers of sterols (20 mol%) in *N*-PSPM were uniformly fluorescent during initial compression when the sterol analogues were *n*-C3, *n*-C4 and *n*-C5 (Fig. 6a–c). The *n*-C6 and *n*-C7 sterols formed laterally condensed domains with *N*-PSPM, these being circular in shape, and much larger and heterogeneous in size with *n*-C6 than with *n*-C7 (Fig. 6d and e). With the single methyl-branched *iso*-series and *N*-PSPM, the *i*-C5 monolayer displayed a homogeneous fluorescence with no lateral domains (Fig. 6f), whereas the rest of the *iso*-sterols formed numerous circular domains. These domains were homogeneous both in size and lateral distribution (Fig. 6g–j), with the exception that the domains in the *i*-C10 monolayer were partly fused (Fig. 6k). When the mixed monolayers had experienced a compression/expansion cycle, the *n*-C7, *i*-C9 and *i*-C10 formed laterally condensed domains which were larger (more fusion) after the cycle

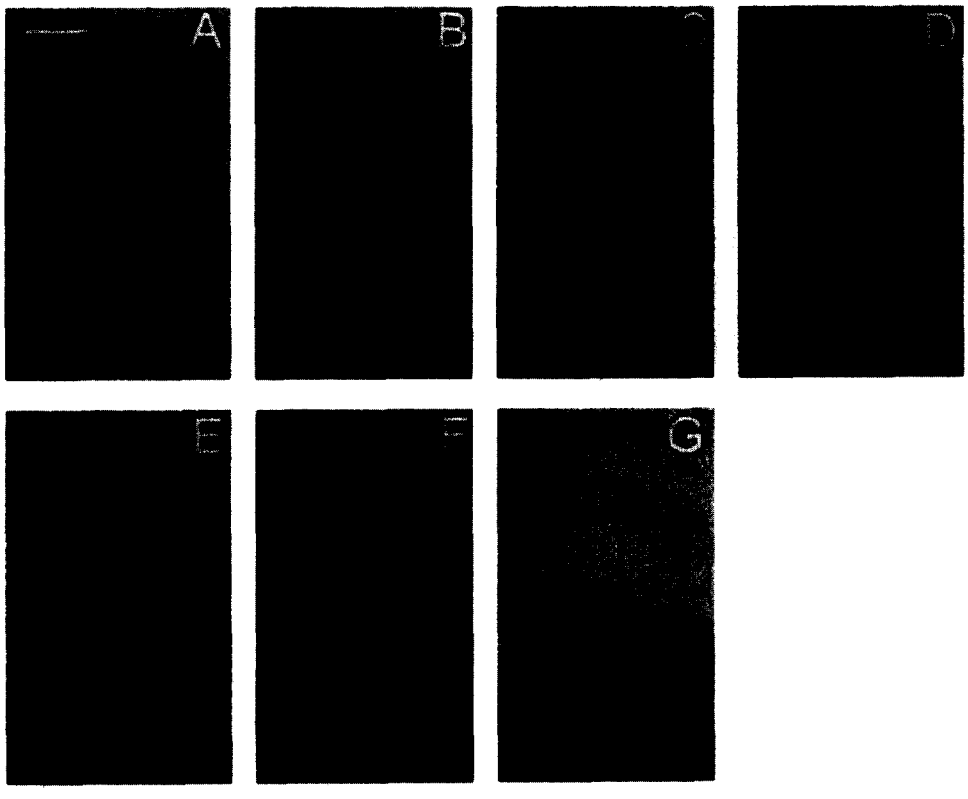

Fig. 5. Phase transformations in a *n*-C5/DPPC monolayer. A monolayer containing 20 mol% *n*-C5, 79 mol% DPPC, and 1 mol% NBD-cholesterol was compressed slowly to 30 mN/m. Micrographs were taken during different stages of the compression, as follows: panel A is at 0.45 mN/m during initial compression, panel B is at 2.0 mN/m, C is at 10.4 mN/m, D id at 30.0 mN/m, E is at 10.5 mN/m during expansion of the monolayer, F is at 2.0 mN/m during expansion, and G is at 0.5 mN/m (expansion). The scale bar is 200 μm.

than before, whereas the surface texture of the other sterol monolayers did not change following a compression/expansion cycle.

The onset phase transformation pressure increased slightly with increasing side chain length for the unbranched sterols (Fig. 7A, solid line), whereas the onset phase transformation pressure was highest with the *i*-C7, *i*-C8, and *i*-C9 sterols, and lower with the other two *iso*-sterol analogues (Fig. 7A, dotted line). When the sterol/*N*-PSPM monolayers were compressed beyond the phase transformation pressure (up to 40 mN/m), no new condensed phases were formed (cf. Fig. 5).

At higher sterol concentration (33 mol%) the monolayer domains were markedly different as compared to the situation with 20 mol% sterol. Whereas the *n*-C3 sterol/*N*-PSPM phospholipid monolayer was uniformly fluorescent with no domains (during initial compression; Fig. 8a), all other unbranched sterol analogues formed laterally condensed domains with *N*-PSPM (Fig. 8b–e). While the *n*-C4 mixed monolayer had small circular-shape liquid-expanded domains of heterogeneous size (Fig. 8b), the *n*-C5, *n*-C6 and *n*-C7 sterol monolayers formed a surface texture with coalesced liquid-expanded and liquid-condensed domains (Fig. 8c–e). Of the single methyl-branched sterol

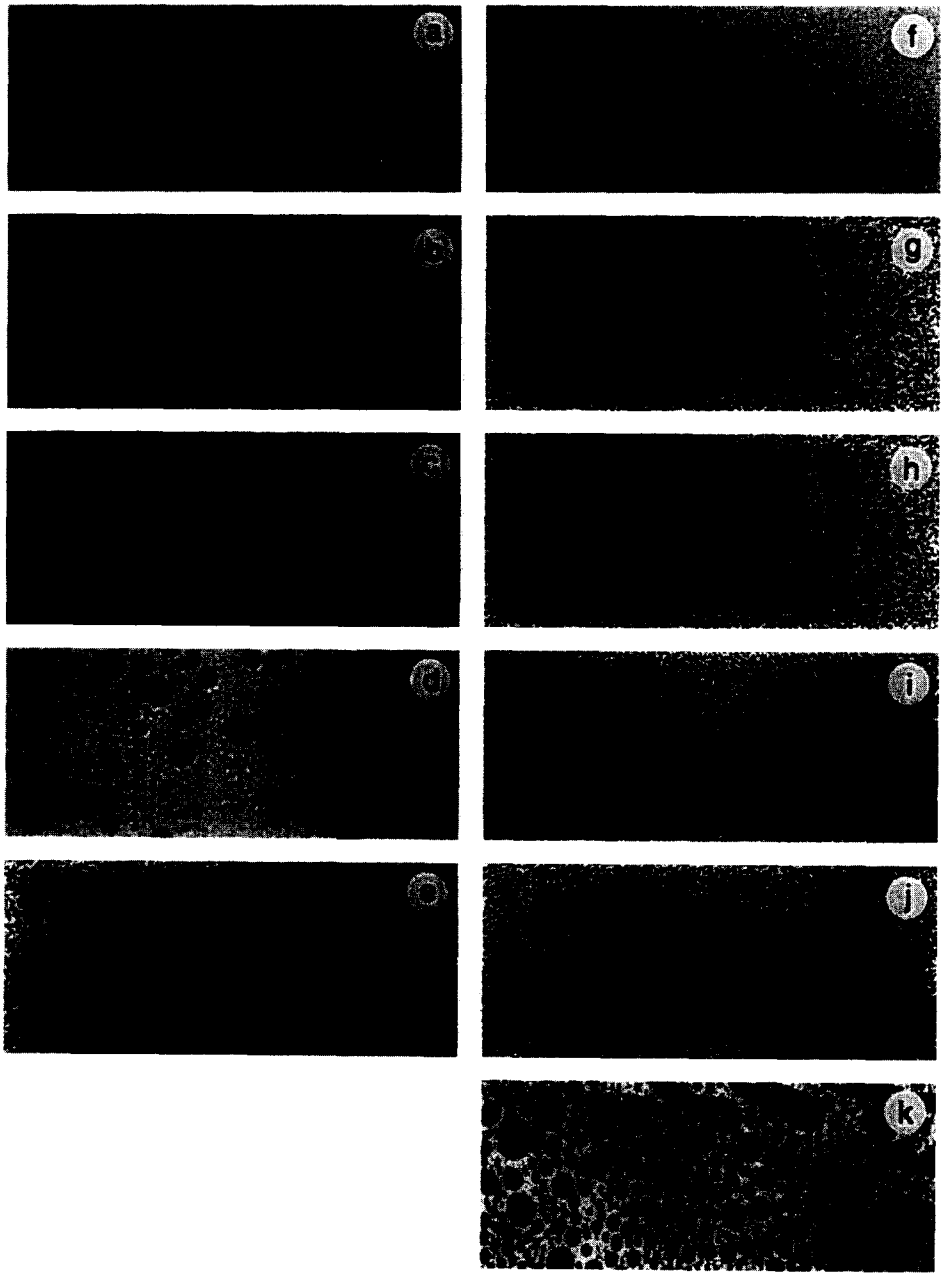

Fig. 6. Lateral domain formation in sterol/*N*-PSPM monolayers. The monolayers contained 20 mol% sterol, 79 mol% *N*-PSPM, and 1 mol% NBD-cholesterol. Micrographs were documented at 0.5 mN/m during the initial compression of the monolayer. Panel a is *n*-C3, b is *n*-C4, c is *n*-C5, d is *n*-C6, e is *n*-C7, f is *i*-C5, g is *i*-C6, h is *i*-C7, i is *i*-C8 (cholesterol), j is *i*-C9, and k is *i*-C10. The scale bar is 100 μm.

analogues, only *i*-C5 failed to form lateral domains (Fig. 8f). All other sterols in the *iso*-series had both liquid-expanded and coalesced liquid-condensed domains which were non-uniformly distributed (Fig. 8g–k).

The shapes of the domains changed surprisingly little when the sterol/*N*-PSPM monolayers were passed through a compression/expansion cycle. The *n*-C4 monolayer had smaller and more uniformly distributed fluorescent inclusions, whereas the other unbranched sterol monolayers remained unchanged. With the branched side chain analogues the compression/expansion cycle triggered the fusion of condensed domains in *i*-C8, *i*-C9 and *i*-C10 containing monolayers, whereas the shorter chain sterol monolayers remained unchanged by the compression/expansion cycle.

At 33 mol% sterol, the onset phase transformation pressure increased markedly with increasing side chain length for the unbranched analogues (Fig. 7B, solid line), whereas the onset phase transformation pressure was highest with the *i*-C8, and *i*-C9 sterols, and lower with the other *iso*-sterol analogues (Fig. 7B, dotted line). The onset phase transformation pressure increased for a given sterol analogue, when its concentration was raised from 20 mol% to 33 mol%.

4. Discussion

The visualization of lateral domains in mixed monolayers by epifluorescence microscopy is possible because certain fluorescent lipid probes (e.g., NBD-cholesterol) partition differently into lateral phases which differ in their packing density and/or long-range order [21,22]. The formation of specific lateral domains in mixed sterol/phospholipid monolayers necessitates the formation of similarly specific molecular associations between the two molecular species. Therefore, the formation of domains can be interpreted to demonstrate the occurrence of a specific interaction between two groups of molecules. However, due to the limited resolution of the light microscope, the absence of visible lateral domains in a mixed monolayer does not rule out the possibility that domains still exist which are too small to be observed by this microscopic technique. The laterally condensed domains formed in a mixed cholesterol/DPPC monolayers are known to be sterol-rich (as opposed to being a pure DPPC domain), because the fractional area of the condensed domains increases with increasing cholesterol concentration [29], and because such domains are not formed in 4-cholesten-3-one/DPPC mixed monolayers [30].

Many different types of model membrane studies have demonstrated the importance of the isooctyl side chain of cholesterol for the optimal interaction of this sterol with various phospholipids [3–8]. In this respect, it is not surprising to find that the side chain composition of the sterols of this study had marked effects on the ability of the sterols to form sterol/phospholipid domains in mixed monolayers. Although all of the sterols used in this study have been previously shown to condense the lateral packing density of both DPPC and 1-stearoyl-2-oleoyl-*sn*-glycero-3-phosphocholine [4], not all of them were able to form macroscopic sterol/phospholipid domains. Based on these results, one can conclude that the ability of a sterol to condense the lateral packing density of a phospholipid is not related to its ability to form lateral sterol/phospholipid domains. This interpretation is further supported by the finding that 3-keto sterols (e.g., 4-cholesten-3-one) cannot form sterol/phosphatidylcholine domains even though they do condense the lateral packing of phospholipids [30].

Sterol analogues with short side chains of both the unbranched (*n*-C3 and *n*-C4) and the single methyl branched type (*i*-C5) were unable to form domains with either DPPC or *N*-PSPM (at a high sterol concentration, the *n*-C4/*N*-PSPM monolayer did show a surface texture indicating possible domain formation). The morphology of the domains formed by the longer side chain analogues

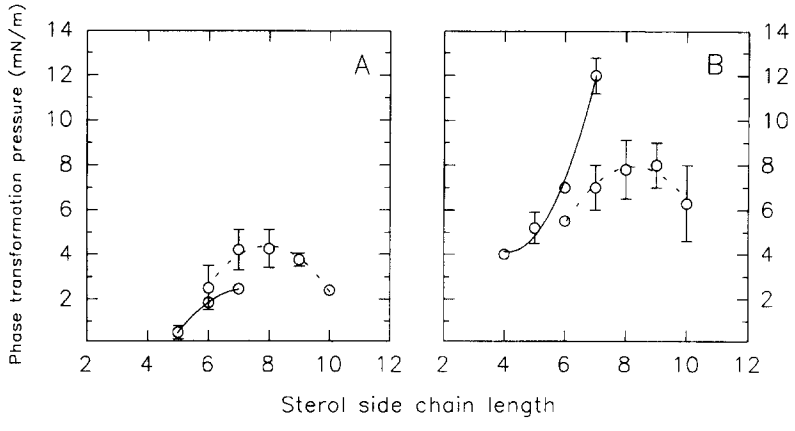

Fig. 7. Onset phase transformation pressure as a function of sterol side chain composition. Sterol/*N*-PSPM mixed monolayers were prepared to contain either 20 (panel A) or 33 (panel B) mol% sterol (together with 1 mol% NBD-cholesterol). The solid line represents sterols from the *n*-series, whereas dotted lines represent *iso*-sterols. Values are averages ± S.E. from three different experiments.

differed somewhat, depending on the length and conformation of the side chain. In general the domains formed in *N*-PSPM mixed monolayers were more homogeneous in size, and more evenly distributed than was the situation in DPPC monolayers. This finding is consistent with our recent data showing a more homogeneous size and lateral distribution of cholesterol/sphingomyelin domains as compared to cholesterol/DPPC domains, when examined as a function of cholesterol concentration [29].

The formation of lateral domains is the result of the interplay of different forces, some of which are attractive (e.g., hydrophobic and van der Waals forces), while other are disruptive (e.g., electrostatic and dipole-induced repulsion; [26,28]). Since all sterols of this study are 3β-hydroxy sterols, the permanent dipole was similar within the sterol series, although the orientation of the overall sterol dipole may differ in a way which possibly depends on the side chain composition, e.g., due to the difference in the angle of the dynamic cone of the rotating sterols [31]. However, it is clear that the strength of sterol/phospholipid association must in part depend on the possibility for attractive van der Waals forces to form. These forces are expected to be more numerous if the sterol side chain is longer rather than shorter. The observation that

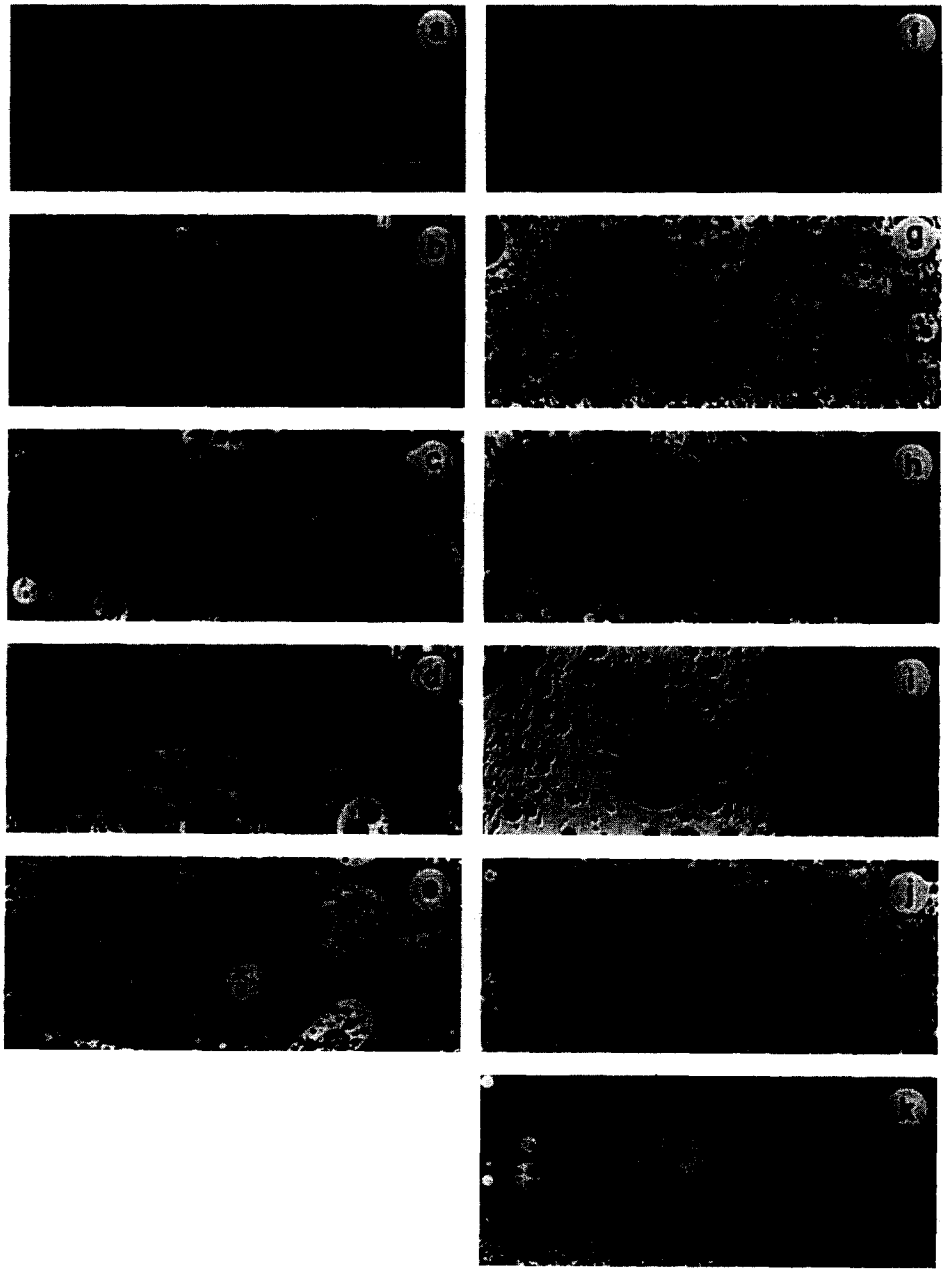

Fig. 8. Lateral domain formation in sterol/*N*-PSPM monolayers. The monolayers contained 33 mol% sterol, 66 mol% *N*-PSPM, and 1 mol% NBD-cholesterol. Micrographs were documented at 0.5 mN/m during the initial compression of the monolayer. Panel a is *n*-C3, b is *n*-C4, c is *n*-C5, d is *n*-C6, e is *n*-C7, f is *i*-C5, g is *i*-C6, h is *i*-C7, i is *i*-C8 (cholesterol), j is *i*-C9, and k is *i*-C10. The scale bar is 100 μm.

sterol/phospholipid domains were formed with intermediate and long side chain sterol analogues, but not with short side chain analogues is consistent with the idea that the formation of lateral domains in some way relates to the formation of an apparently critical number of attractive van der Waals forces. This in turn may relate to a phenomenon of hydrophobic mismatch that has been described for bilayer membrane containing, e.g., DPPC and sterols with different length side chains [32,33]. In the study of McMullen et al. [32], using similar sterol analogues that we have used in this study, it was shown that whereas the *n*- or *iso*-configuration of the side chain did not alter the thermotropic phase behavior of DPPC, even small changes in the length of the C17 linked side chain had marked effects on the phase behavior of the bilayers. This behavior of the sterols was described to arise from the hydrophobic mismatch between different sterols and DPPC [32].

It is well established that the lateral domains formed in mixed cholesterol/phospholipid monolayers are stable only within a specific surface pressure range ([18,19,26], this study). If the monolayer surface pressure is increased to a certain level (onset phase transformation pressure), the domain line boundary dissipates, bringing the monolayer from a two-phase coexistence into an apparent one-phase system. Immediately below the phase transformation pressure, both the attractive (hydrophobic and van der Waals) and the repulsive (electrostatic and dipole-induced repulsion) forces are balanced, but as the monolayer is further compressed, the repulsive interactions begin to dominate over the attractive forces, and as a consequence, the domain wall energy disappears [26,28]. This eventually leads to the dissipation of the domain line boundary. This phase transformation pressure, at which the domain line boundary dissipates, can also be deduced from an analysis of the force–area isotherm, as has been suggested previously in [26]. The agreement between the phase transformation pressure obtained by visual observation and by isotherm analysis is generally excellent [34]. The characteristic onset phase transformation pressure was a clear function of sterol side chain composition. However, the interpretation of the results is complicated by the finding that the onset phase transformation pressure appears to be differently sensitive to the sterol concentration in monolayers with unbranched and methyl-branched side chain analogues, and also differs from the DPPC to the *N*-PSPM system.

Although monolayer membranes turn into an apparent one-phase state when the surface pressure is raised above the phase transformation pressure, it is still likely that a heterogeneous distribution of sterols in the plane of the membrane remains. Different experimental approaches using bilayer membranes as models have shown that the lateral distribution of cholesterol in phospholipid membranes is laterally heterogeneous [35–37]. These findings suggest that cholesterol-rich domains (although not similar to those we observed in monolayers at low surface pressures) can exist at the higher surface pressures of bilayer membranes. The surface pressure of biological and model membranes have been estimated to be in the range of 15–35 mN/m [38–41].

An additional feature of this study was the formation of a specific condensed phase in certain short-chain sterol/DPPC monolayers (at 20 mol%) above the phase transformation pressure. It was found that a new condensed phase appeared to precipitate at surface pressures above the phase transformation pressure in monolayers of DPPC and the *n*-C3, *n*-C4, *n*-C5, and *i*-C5 analogues, but not in the *N*-PSPM mixed monolayers. We do not know whether these condensed domains represent a pure lipid aggregate (of sterol or DPPC) or whether they result from a sterol/DPPC interaction. However, it is apparently more likely that the condensed phase may represent a pure DPPC phase. Albrecht and coworkers [25] have prepared a phase diagram of a binary mixture of cholesterol and DPPC, and have shown that at 20 mol% sterol and at pressure above 11 mN/m, the monolayer should include a phase containing almost pure phospholipid. In a recent differential scanning calorimetry study of sterol miscibility in DPPC bilayers it was shown that partial immiscibility of sterols in the DPPC host membrane may arise if the hydrophobic mismatch between the sterol length and the DPPC length is too great [32]. In fact it was shown that the *i*-C3 and *i*-C5 sterols did not completely eliminate the DPPC chain-melting transition even at 50 mol%, suggesting partial immiscibility [32]. In light of the results reported by McMullen et al. [32] it is therefore likely that the condensed precipitate seen in DPPC monolayers containing one of the sterols *n*-C3 to *n*-C5 and *i*-C5 was pure DPPC, which would be expected to crystallize at surface pressures above 4–6 mN/m (at 22°C). Since short-chain sterols interact less favorably with DPPC than longer chain sterols, it appeared that their capacity to prevent DPPC form crystallizing is reduced. However, it should again be noted that the visual observation of condensed phases above the phase transformation pressure in some sterol/phospholipid mixtures does not exclude the possibility that similar but visually non-resolvable phases also may have occurred in the other mixed monolayers.

In conclusion, this study has examined the effect of varying the sterol side chain composition on the formation of laterally segregated sterol-rich domains in mixed monolayers of either DPPC or *N*-PSPM. From the results obtained it can be concluded that van der Waals forces acting between the acyl chains of the phospholipids and the sterol molecules, including the side chain, are important in determining the lateral distribution, as well as the solubility of sterols in these phospholipid membranes.

Acknowledgements

This study was supported by generous grants from the Academy of Finland, the Sigrid Juselius Foundation, and

the Åbo Akademi University (P.M. and J.P.S.), and NIH HL-16660 (R.B.).

References

[1] Yeagle, P.L. (1993) in Cholesterol in Model Membranes (Finegold, L.X., ed.), pp. 1–12, CRC Press, Boca Raton.
[2] Demel, R.A., Bruckdorfer, K.R. and Van Deenen, L.L.M. (1972) Biochim. Biophys. Acta 255, 321–330.
[3] Demel, R.A., Geurts van Kessel, W.S.M. and Van Deenen, L.L.M. (1972) Biochim. Biophys. Acta 266, 26–40.
[4] Slotte, J.P., Jungner, M., Vilchéze, C. and Bittman, R. (1994) Biochim. Biophys. Acta 1190, 435–443.
[5] Nakamura, T., Nishikawa, M., Inoue, K., Nojima, S., Akiyama, T. and Sankawa, U. (1980) Chem. Phys. Lipids 26, 101–110.
[6] Suckling, K.E. and Boyd, G.S. (1976) Biochim. Biophys. Acta 436, 295–300.
[7] Craig, I.F., Boyd, G.S. and Suckling, K.E. (1978) Biochim. Biophys. Acta 508, 418–421.
[8] Suckling, K.E., Blair, H.A.F., Boyd, G.S., Craig, I.F. and Malcolm, B.R. (1979) Biochim. Biophys. Acta 551, 10–21.
[9] Clejan, S. and Bittman, R. (1985) J. Biol. Chem. 260, 2884–2889.
[10] Clejan, S. and Bittman, R. (1984) J. Biol. Chem. 259, 449–455.
[11] Wilson, M.D. and Rudel, L.L. (1994) J. Lipid Res. 35, 943–955.
[12] Kan, C.-C. and Bittman, R. (1990) J. Am. Chem. Soc. 112, 884–886.
[13] Kan, C.-C. and Bittman, R. (1991) J. Am. Chem. Soc. 113, 6650–6656.
[14] Mattjus, P. and Slotte, J.P. (1994) Chem. Phys. Lipids 71, 73–81.
[15] Slotte, J.P. (1992) Biochemistry 31, 5472–5477.
[16] McIntosh, T.J., Simon, S.A., Needham, D. and Huang, C.-h. (1992) Biochemistry 31, 2012–2020.
[17] Bittman, R., Kasireddy, C.R., Mattjus, P. and Slotte, J.P. (1994) Biochemistry 33, 11776–11781.
[18] Subramaniam, S. and McConnell, H.M. (1987) J. Phys. Chem. 91, 1715–1718.
[19] Rice, P.A. and McConnell, H.M. (1989) Proc. Natl. Acad. Sci. USA 86, 6445–6448.
[20] Weis, R.M. (1991) Chem. Phys. Lipids 57, 227–239.
[21] Von Tscharner, V. and McConnell, H.M. (1981) Biophys. J. 36, 409–419.
[22] Lösche, M., Sackmann, E. and Möhwald, H. (1983) Ber. Bunsen-Ges. Phys. Chem. 87, 848–852.
[23] Slotte, J.P. and Mattjus, P. (1994) Biochim. Biophys. Acta 1254, 22–29.
[24] Mattjus, P., Hedström, G. and Slotte, J.P. (1994) Chem. Phys. Lipids 74, 195–203.
[25] Albrecht, O., Gruler, H. and Sackmann, E. (1981) J. Colloid. Interf. Sci. 79, 319–388.
[26] Seul, M. and Sammon, M.J. (1990) Phys. Rev. Lett. 64, 1903–1906.
[27] Yu, H. and Hui, S.W. (1992) Chem. Phys. Lipids 62, 69–78.
[28] Keller, D., Korb, J.P. and McConnell, H.M. (1987) J. Phys. Chem. 91, 6417–6422.
[29] Slotte, J.P. (1995) Biochim. Biophys. Acta 1235, 419–427.
[30] Slotte, J.P. (1995) Biochim. Biophys. Acta 1237, 127–134.
[31] Gallay, J. and De Kruijff, B. (1982) FEBS Lett. 143, 133–136.
[32] McMullen, T.P.W., Vilchèze, C., McElhaney, R.N. and Bittman, R. (1995) Biophys. J. 69, 169–176.
[33] Chia, N.-C., Vilchèze, C., Bittman, R. and Mendelsohn, R. (1993) J. Am. Chem. Soc. 115, 12050–12055.
[34] Slotte, J.P. (1995) Biochim. Biophys. Acta 1238, 118–126.
[35] Schroeder, F., Jefferson, J.R., Kier, A.B., Knittel, J., Scallen, T.J., Wood, W.G. and Hapala, I. (1991) Proc. Soc. Exp. Biol. Med. 196, 235–252.
[36] Rubinstein, J.L.R., Owicki, J.C. and McConnell, H.M. (1980) Biochemistry 19, 569–573.
[37] Ben-Yashar, V. and Barenholtz, Y. (1989) Biochim. Biophys. Acta 985, 271–278.
[38] Demel, R.A., Geurts van Kessel, W.S.M., Zwaal, R.F.A., Roelofsen, B. and Van Deenen, L.L.M. (1975) Biochim. Biophys. Acta 406, 97–107.
[39] Ibdah, J.A., Lund-Katz, S. and Phillips, M.C. (1989) Biochemistry 28, 1126–1133.
[40] Slotte, J.P. and Grönberg, L. (1990) J. Lipid Res. 31, 2235–2242.
[41] Small, D.H. and Phillips, M.C. (1992) Adv. Coll. Interface Sci. 41, 1–8.